# The Actuation Behavior and Stability of *p*-Toluene Sulfonate Doped Polypyrrole Films Formed at Different Deposition Current Densities

**Jing Sui, Jadranka Travas-Sejdic, Shu Yi Chu, Kwong Chi Li, Paul A. Kilmartin**

*Chemistry Department, Polymer Electronics Research Group, The University of Auckland, Private Bag 92019, Auckland, New Zealand*

Received 6 June 2008; accepted 18 August 2008
DOI 10.1002/app.29119
Published online 16 October 2008 in Wiley InterScience (www.interscience.wiley.com).

**ABSTRACT:** Free-standing films of polypyrrole doped with *p*-toluene sulfonate (PPy/pTS) were electropolymerized galvanostatically at different deposition current densities and their electrochemomechanical deformation (ECMD) properties were measured *in situ* during cyclic voltammetry experiments. It was found that films exhibiting a higher cation-driven actuation strain were generated when a lower current density was used in electropolymerization, which also led to an increase in PPy conductivity and doping level. A decrease in cation-driven strain with time was observed in all cases due to a loss of pTS anions from the films. Raman, FTIR, and elemental analyses were used to characterize the films grown at different deposition current densities and no sign of excessive overoxidation was found. SEM images revealed that the morphology of the films was affected by the current density during electropolymerization.
© 2008 Wiley Periodicals, Inc. J Appl Polym Sci 111: 876–882, 2009

**Key words:** polypyrrole films; strain; electropolymerization; current density

## INTRODUCTION

Inherently conducting polymers, such as polypyrrole, polyaniline, and polythiophene, have the ability to undergo reversible redox reactions with simultaneous changes in properties such as conductivity, color, and volume. Conducting polymers are promising materials for several applications including batteries,[1] super capacitors,[2] electrochemical sensors,[3] and mechanical actuators.[4]

Polypyrrole is one of the most extensively investigated conducting polymers for application as an actuator because of the large volume changes which have been observed, along with high mechanical strength,[5] conductivity,[6] good environmental stability,[7] and the simple preparation required.[8] Polypyrrole can be prepared via chemical or electrochemical polymerization.[9] The volume change of polypyrrole is related to movement of ions between the polymer chains during redox doping processes. If the polymer is prepared with a small, mobile anion, the polymer expands at the oxidized state. However, for a PPy polymer prepared with a large, immobile anion, the polymer expands at the reduced state.[10]

*Correspondence to:* P. A. Kilmartin (p.kilmartin@auckland.ac.nz).

Journal of Applied Polymer Science, Vol. 111, 876–882 (2009)
© 2008 Wiley Periodicals, Inc.

Electrochemical polymerization has the advantage in that it provides better control of film thickness and morphology and forms purer polymers compared with chemical oxidation.[11] The preparation conditions for producing PPy films, including electrolyte,[12] solvent,[13] pH,[14] temperature,[15] and electrochemical method[16,17] greatly influence the morphology, conductivity, electrochemical characteristics, and mechanical properties of the conducting polymer.

Polypyrrole prepared with *p*-toluene sulfonate (pTS) is an extensively investigated form of polypyrrole. Okamoto reported that PPy/pTS cylindrical films prepared in a Teflon pipe could show bending behavior.[18] Kagawa et al.[19] reported PPy/pTS films prepared by using an amphiphilic template which displayed superior electroactivity and ion diffusion and higher actuation strain compared with typical polypyrrole. Recently, Ochoteco et al.[20] reported a simplified bilayer actuator assembled using PPy/pTS and PPy/$ClO_4$, which showed no evidence of delamination after multiple cycles. PPy/pTS has proven to be very promising for practical applications because of its good physical, chemical, and mechanical properties and high conductivity.[21] However, the influence of preparative conditions on the actuation properties of PPy/pTS films have not been examined. In this report, we examine the ECMD response of PPy films prepared and tested in aqueous sodium *p*-toluene sulfonate (NapTS), as a

function of deposition current density. The PPy films have been characterized using electrochemical methods, scanning electron microscopy, along with Raman and FTIR spectroscopies.

## EXPERIMENTAL

### Materials

Sodium *p*-toluene sulfonate (NapTS) was purchased from Aldrich Chemical (St. Louis, MO) and used as supplied. Pyrrole (Aldrich) was freshly distilled before use. Milli-Q water, with a resistance of at least 18$M\Omega$ $cm^{-1}$, was used to prepare aqueous electrolytes.

### Methods

PPy freestanding films were prepared by electropolymerization from an aqueous solution containing 0.1*M* of freshly distilled pyrrole and 0.1*M* of NapTS. The electropolymerization was performed on a 2.4 $cm^2$ stainless steel (SS) working electrode at current densities from 0.1 to 2.0 mA $cm^{-2}$ with a three-electrode cell assembly, including a platinum foil counter electrode and Ag/AgCl (3*M* KCl) reference electrode. The aqueous electrolyte containing the pyrrole monomer was purged with nitrogen gas for 15 min before the initiation of electropolymerization. The polymerization time was adjusted considering the current density until the charge reached 3.0 C $cm^{-2}$, which corresponds to a film thickness of about 15 μm.[22] The temperature for electropolymerization was kept at 2 ± 1°C.

The ECMD responses of the freestanding films (10 mm in length and 2 mm in width) were studied using a Dynamical Muscle Analyzer from Aurora Scientific Inc. (ASI) (Model 300B Dual-Mode Lever Arm System) during cyclic voltammetry (CV). The top-end of the PPy strip was clamped between two PEEK plates that hung on a wire attached to the lever arm, whereas the bottom end of the strip was fixed to a polyvinyl chloride holder with a Pt wire as the electrical contact. The typical length of the PPy films between the clamps was 2 mm. A small constant force (60 mN) was applied to the film at the beginning of the measurement.

The PPy strip was immersed in a cell containing 0.1*M* NapTS (aq.) and a Pt sheet was used as the counter electrode and Ag/AgCl as the reference electrode. The electrolyte was purged with nitrogen before actuation testing. CV traces were measured at a scan rate of 10 mV $s^{-1}$, cycling between −0.8 V and +0.6 V. The deformation magnitude was defined by $\Delta l/l_0$ (strain) in %, where $l_0$ and $\Delta l$ are original length and the change in the film length (during reduction), respectively.

The conductivity of dry, free standing polymer films was measured using a four-probe conductivity meter (Model RM2, Jandel 4-Point Probe head). The conductivity was measured on several different areas on the front side of the polymer films.

Raman spectra were recorded using a Renishaw 1000 Raman spectrophotometer employing a 785 nm laser beam. As-grown PPy films were washed repeatedly with acetone and deionized water to remove the electrolyte and the monomer and finally dried at room temperature before Raman characterization. Twenty spectra were recorded with 20 $cm^{-1}$ resolution and the power was always kept very low to avoid destruction of the samples. FTIR spectra were recorded using a BioRad FTS 60 FTIR transmission mode spectrophotometer.

The surface morphology of the PPy films was examined using a Philip ML30S FEG scanning electron microscope. Sample charging effects were minimized by applying a thin coating of platinum on the films before analysis. The images were measured using a 5 keV electron beam with a spot size of 3 nm.

## RESULTS AND DISCUSSION

### Electropolymerization

To investigate the effect of current density during film deposition, both the concentration of pyrrole and NapTS were kept constant at 0.1*M*, whereas the deposition current density was varied from 0.1 to 2.0 mA $cm^{-2}$. The application of current to the electrode increased the potential sharply to a maximum value in all cases, assumed to be due to a change of surface potential accompanied by formation of the first PPy nuclei. Once the nucleation process was completed, the potential decreased to steady values in a few seconds between 0.65 V (for the 0.1 mA $cm^{-2}$ deposition) to 0.9 V (2.0 mA $cm^{-2}$ deposition) (Fig. 1). Over the course of the polymerization (between 1500 and 30,000 s depending on the currents used), a very gradual increase in potential was seen. This would be due to a decreasing concentration of pyrrole monomer and newly formed oligomers near the surface of the electrode, a diffusion controlled process,[23] and the resistance of the growing PPy film. As the current density was increased, more monomers in the solution were converted to oligomers, which required a higher electrode potential to drive the process.[24]

### Electrochemomechanical deformation during cyclic voltammetry

PPy/pTS films polymerized at different current densities were cycled nine times in the potential range

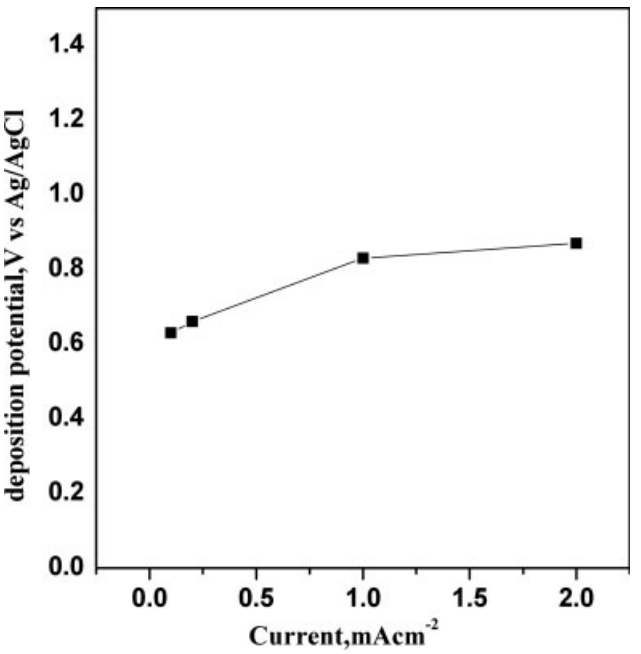


**Figure 1** Polymerization potential as a function of deposition current density during electropolymerization of PPy/pTS films.

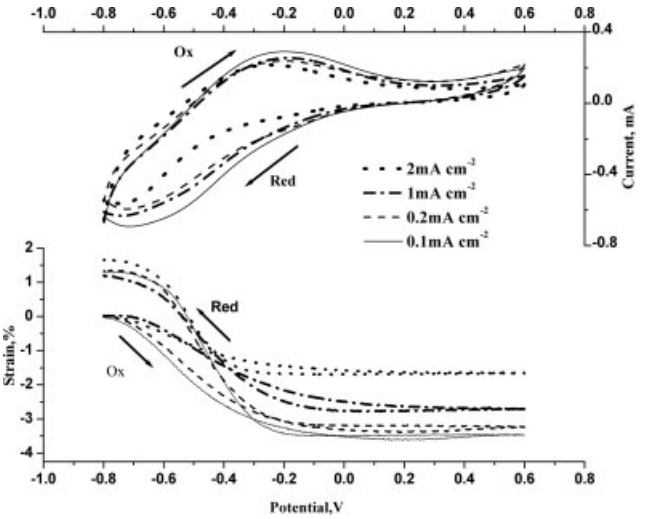


**Figure 2** Cyclic voltammograms and ECMD curves during the second cycle for PPy/pTS polymerized at different current densities, and cycled in aqueous 0.1M NapTS between −0.8 V and + 0.6 V at a scan rate of 10 mV $s^{-1}$.

from −0.8 V and +0.6 V (versus Ag/AgCl) at 10 mV $s^{-1}$ in an aqueous solution of 0.1*M* NapTS. Figure 2 presents the cyclic voltammograms and associated electrochemomechanical deformation (ECMD) curves during the 2nd cycle. In general, PPy/pTS films mainly show cation-driven actuation at a more negative potential, at potentials less than −0.2 V. Oxidation waves were seen during CV scans at approximately −0.2 V and reduction waves at −0.7 V. The deposition current density had little effect on the shape of the cyclic voltammograms, but the CV current decreased for films formed using a higher polymerization current, with much lower CV currents seen in the 2 mA $cm^{-2}$ case, pointing to less electroactive PPy material. The values for the charge passed on the reduction step are summarized in Table I, showing that more electroactive films (higher charge passed) were formed using a lower deposition current density.

Regarding the measured strains in the ECMD curves (Fig. 3), all of films generated the highest strain in the first cycle. This phenomenon has been explained by changes in polymer morphology on the first scan, and more particular, for systems dominated by cation movement, by the first-time entry of cations where only large anions had been included in the film during polymerization.[25,26] Films prepared from the highest current density (2 mA $cm^{-2}$) showed an average strain of 6.4% during the first cycle. By contrast, films prepared at 0.1 mA $cm^{-2}$ showed a higher strain for each cycle number and an average strain in the first cycle of 7.1%. On the other hand, all films remained mainly cation-driven actuation behavior with continued scanning, but a considerable decrease in strain over time was observed for all samples. The average strain for the film polymerized at 2 mA $cm^{-2}$ dropped to 3.6% for the second cycle and then to 1.8% by the ninth cycle. As for films polymerized at 0.1 mA $cm^{-2}$, the average strains in the second and last cycles were 4.8% and 2.9%, respectively.

Despite the steady decrease in strain, films polymerized at a lower current density generated a higher average strain at each cycle number. The results for the consumed charge on the reduction process (Table I), which indicate that a lower current density generated more electroactive films,[27] are

**TABLE I**
**Strains and Consumed Charges at the 2nd and 9th Reduction Cycles**

| Current density (mA $cm^{-2}$) | Charge (mC) 2nd cycle | Strain 2nd cycle | Strain/charge 2nd cycle | Charge (mC) 9th cycle | Strain 9th cycle | Strain/charge 9th cycle |
|---|---|---|---|---|---|---|
| 2 | −0.0241 | 3.6% | −1.50 | −0.0148 | 1.8% | −1.21 |
| 1 | −0.0296 | 4.2% | −1.41 | −0.0213 | 2.5% | −1.17 |
| 0.2 | −0.0312 | 4.6% | −1.47 | −0.0225 | 2.7% | −1.20 |
| 0.1 | −0.0329 | 4.9% | −1.45 | −0.0234 | 2.9% | −1.23 |

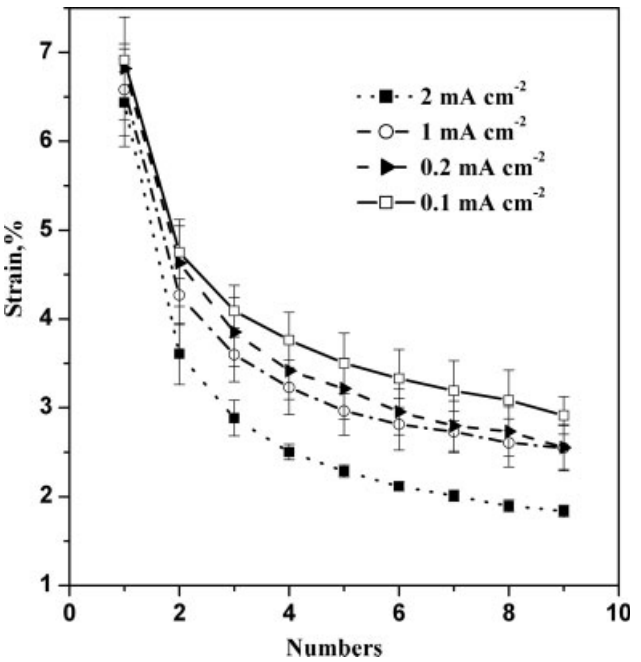


**Figure 3** Average strains upon reduction for PPy/pTS films deposited at different current densities and cycled in 0.1*M* NapTS between −0.8 V and +0.6 V at a scan rate of 10 mV $s^{-1}$, as a function of cycle number ($n = 3$).

consistent with the larger strains exhibited by samples deposited at a lower current density. At the same time, the strain to charge ratios on both the second and ninth scans (Table I) were similar for the different PPy films. It has been shown that a low current density is expected to lead to a lower concentration of oxidized pyrrole monomers at the surface of the growing PPy films.[24] Therefore, at a lower deposition current density, the route for the polymerization has a higher probability for radical–neutral coupling than for radical–radical coupling. This could reduce the number of defects and lead to longer polymer chains[28] and formed films with better qualities.

As discussed earlier, PPy/pTS films mainly showed actuation strain at more negative potentials, below −0.2 V. However, solvent reduction is more likely to happen at the lower potentials in an aqueous solvent, which might lead to degradation of films.[29] In addition, the diffusion and gradual loss of bulky pTS anions out of the PPy films can also contribute to a decrease in strain values. With less pTS anions within the films, a smaller ingress of cations was required during the redox processes, leading to a lower cation-driven actuation with time. Gandhi et al.[30] reported that pTS anions can diffuse from the polymer in the form of $pTS^-/A^+$(small cation) ion pairs. This process was dubbed "salt draining," and occurred easily in electrolytes which had small anions. At the same time, the consistent decrease in the strain to charge ratio from the second to the ninth cycles (Table I) points to a lowering in the efficiency of the actuation, compared with the amount of charge being passed, in all of the films.

To further understand the nature of the pTS anion, the same PPy film was cycled in NapTS and $NaPF_6$, respectively, in the potential range from the −1.0 V to +0.6 V at a lower scan rate of 2 mV $s^{-1}$. Previous studies using PPy/pTS have shown that when the film is cycled in a new electrolyte containing smaller anions that exchange of some of the pTS anions can occur.[31] A more negative potential −1.0 V was selected to get full information about the CV and ECMD response, although solvent reduction is more likely to occur at this potential. The results are shown in Figure 4. As can seen, the CV of PPy/pTS

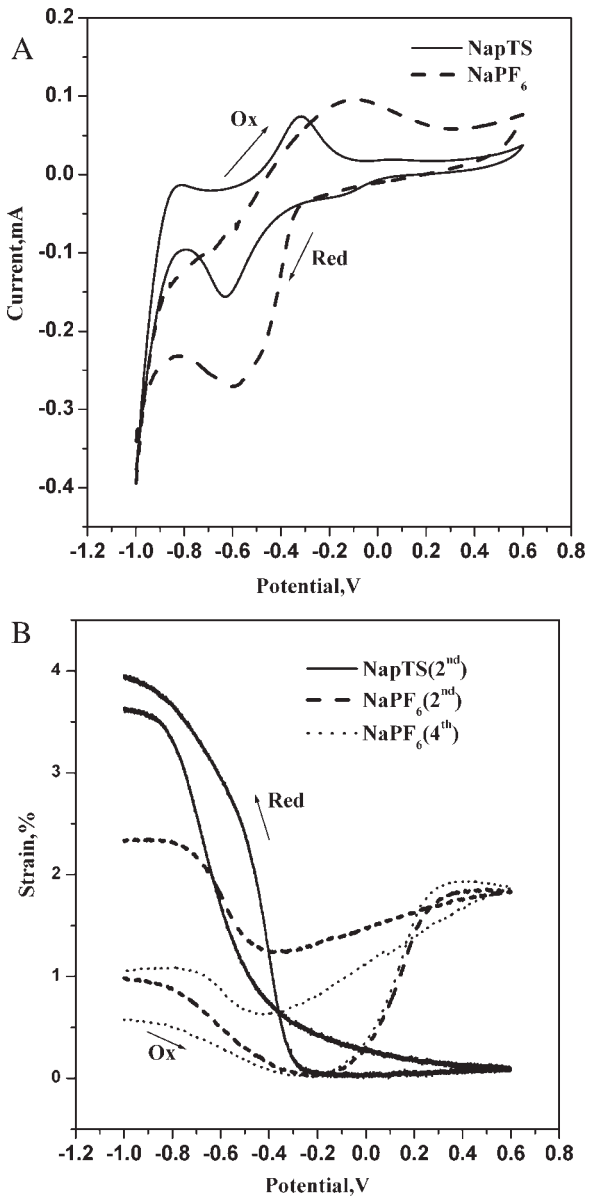


**Figure 4** Cyclic voltammograms (A) and ECMD curves (B) for PPy/pTS films polymerized at 2 mA $cm^{-2}$, and cycled in aqueous 0.1*M* NapTS (2nd cycle) and 0.1*M* $NaPF_6$ (2nd and 4th cycle) between −1.0 V and +0.6 V at a scan rate of 2 mV $s^{-1}$.

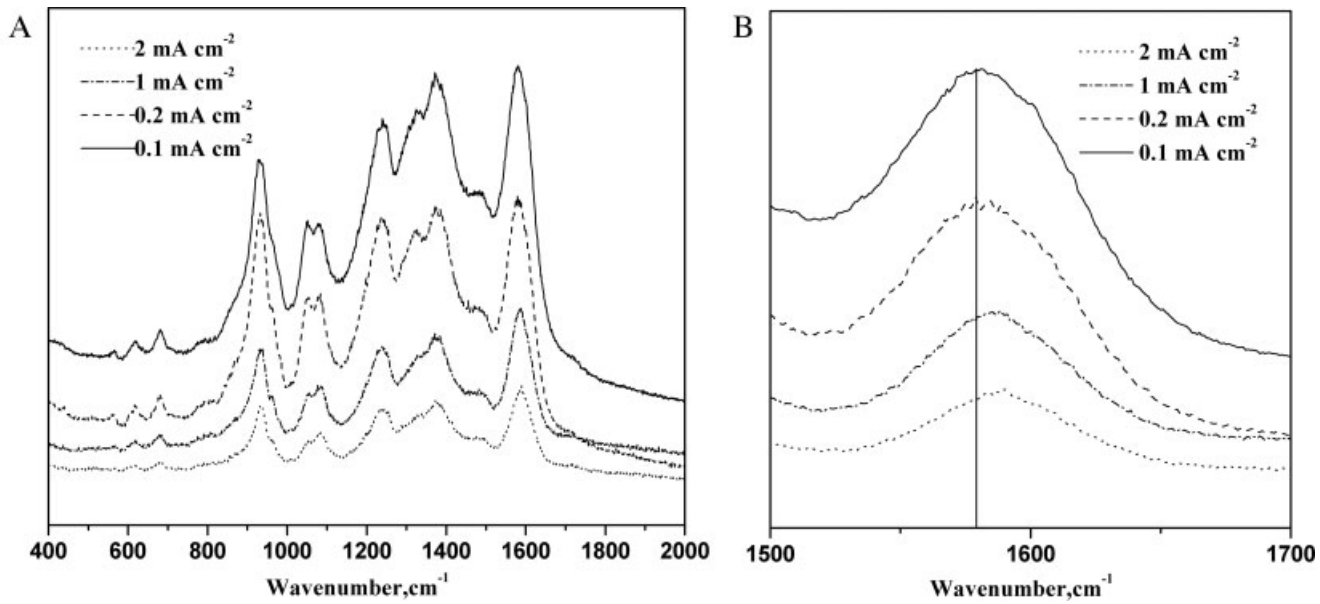


**Figure 5** Raman spectra of as-grown PPy/pTS films polymerized at different current densities.

in $NaPF_6$ shows a reduction wave at approximately −0.6 V and an oxidation wave at approximately −0.11 V [Fig. 4(A)]. Thus the potential difference between the oxidation and reduction peaks ($\Delta Ep$) is calculated to be 0.49 V, larger than that in the case of in NapTS (0.32 V). This result demonstrated that the reversibility of the electrochemical process of PPy/pTS in $NaPF_6$ has decreased.[32] Furthermore, a positive length change in films was seen at both anodic (1.8%) and cathodic potentials (1.1%) in $NaPF_6$ in contrast to the mainly unidirectional actuation, driven by diffusion of solvated cations ($Na^+$), in NapTS [Fig. 4(B)]. With continued cycling, the extent of cathodic actuation progressively decreased, as seen in the ECDM response after four cycles [Fig. 4(B)]. The dual actuation mode in $NaPF_6$ demonstrates that the pTS anions initially incorporated within the films can partly move out the polymer chains and be exchanged by small anions such as $PF_6^-$. Therefore, the movement of $Na^+$ dominates the actuation behavior of the PPy/pTS films in an NapTS electrolyte, as the size of $Na^+$ is much smaller than pTS.[30] However, some of the pTS anions still can move slowly out the film leading to decreased cation-driven actuation over time.

### Structural characterization and surface morphology

PPy films deposited at different current densities were characterized using IR, Raman, and elemental analyses. In general, the PPy films showed similar IR spectra, typical of polypyrrole. The peak attributed to a carbonyl group, often seen around 1700 $cm^{-1}$, was not observed with any of the films,[33] indicating that these films were not greatly overoxidized.

Raman spectra obtained for the four PPy/pTS films (Fig. 5) also matched those reported previously for typical PPy.[34–36] The strong band located at approximately 1580 $cm^{-1}$ represents the C=C backbone stretching of PPy. The double peaks at about 1050 and 1080 $cm^{-1}$ are assigned to a C—H in-plane deformation. The other double peaks at approximately 1320 $cm^{-1}$ and 1380 $cm^{-1}$ are attributed to the ring-stretching mode of PPy. The bands at 927 $cm^{-1}$ and 1240 $cm^{-1}$ are attributed to the CH out-of-plane bending of oxidized PPy and C—H or N—H in plane bending respectively. On closer examination of the main C=C stretching vibration, the peak position was seen to move from 1588 $cm^{-1}$ for PPy (2 mA $cm^{-2}$) through to 1580 $cm^{-1}$ for PPy (0.1 mA $cm^{-2}$) [Fig. 5(B)]. As reported in the literature,[28,37] the C=C peak is related to the conjugation length of PPy and the doping level. This peak shifts to a higher wave number if PPy is present at a lower doping level or contains shorter PPy chain lengths,

**TABLE II**
**Elemental Analysis Results for PPy Films Polymerized at Different Current Densities**

| Current density (mA $cm^{-2}$) | 2 | 1 | 0.2 | 0.1 |
|---|---|---|---|---|
| C (mass %) | 58.2 | 58.54 | 58.73 | 58.3 |
| H (mass %) | 4.46 | 4.54 | 4.75 | 4.43 |
| N (mass %) | 10.9 | 10.9 | 10.7 | 10.57 |
| S (mass %) | 7.48 | 7.73 | 7.84 | 7.92 |
| Doping level [$N^+/N$ = S/N (mol)] | 0.30 | 0.31 | 0.32 | 0.32 |
| Conductivity (S $cm^{-1}$) | 97 | 128 | 328 | 351 |

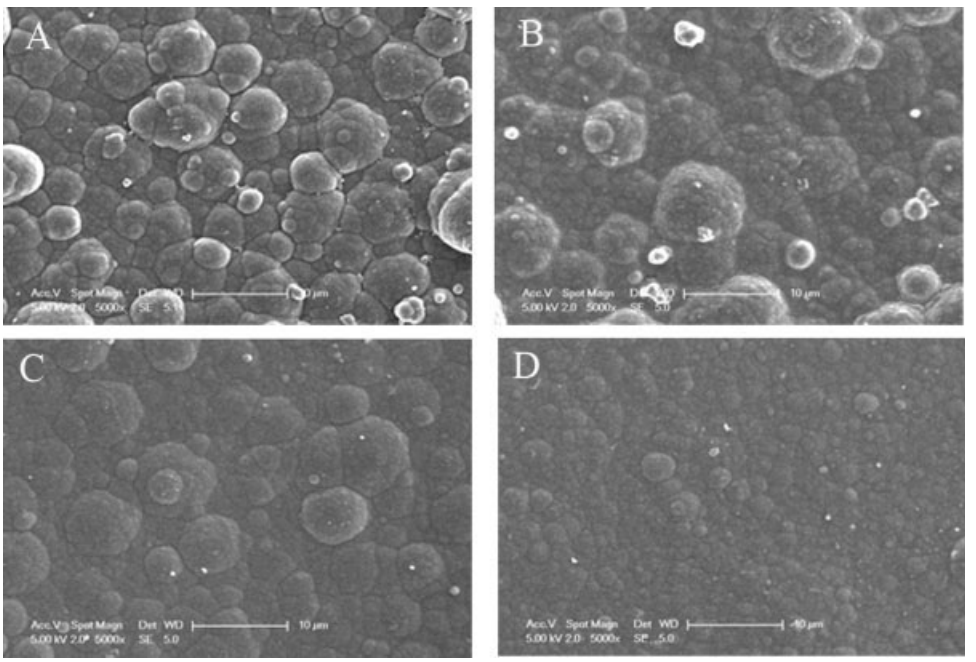


**Figure 6** Surface morphology of PPy/pTS films polymerized at different current densities: (A) 2 mA $cm^{-2}$, (B) 1 mA $cm^{-2}$, (C) 0.2 mA $cm^{-2}$, (D) 0.1 mA $cm^{-2}$.

which might be the case for the PPy prepared at a higher deposition current density.

Table II shows the results of the elemental analyses for the PPy films including the molar percentage of $N^+/N$. In each case, the $N^+/N$ ratio was calculated based on the molar ratios of sulfur to nitrogen.[38] It can be seen that a decrease in deposition current density resulted in a slight increase in the doping level. At the highest current density (2 mA $cm^{-2}$), the $N^+/N$ ratio of the film was 0.30. When the current density was decreased to 0.1 mA $cm^{-2}$, the $N^+/N$ ratio of the film increased to 0.33. At the same time, decreasing the polymerization current density from 2 to 0.1 mA $cm^{-2}$ resulted in an increased conductivity of the films from 97 to 351 S $cm^{-1}$ (Table II). As discussed earlier, a lower polymerization potential was generated when a lower deposition current density was used, which would minimize polymer degradation and the formation of "disordered" chains (interchain links, side chains, or chain terminations),[39] thus producing a polymer of a higher quality. Therefore, films deposited at a lower current density showed greater electrochemical activity and a higher actuation strain.

Figure 6 shows the surface morphology of PPy/pTS films (solution facing side) polymerized at different current densities. A perusal of the SEM micrographs suggests that the morphology of the films is significantly affected by the deposition current density. PPy films polymerized at a high current density typically showed a rough microglobular surface. On the other hand, films polymerized at a low current density showed a more smooth and compact surface. Meanwhile, the average diameter of microglobular forms of PPy decreased from 3.7 μm at 2 mA $cm^{-2}$ to 1.3 μm at 0.1 mA $cm^{-2}$. This could be due to the effect of different electropolymerization rates. At a high current density, films grow at a faster rate which results in a rough and nonuniform morphology, which may be less suitable for ion movement and large actuation strains.[40]

## CONCLUSIONS

Results obtained for PPy/pTS films prepared at different deposition current densities indicated that higher actuation strains were generated when a lower current density (0.1 to 2.0 mA $cm^{-2}$ range) was used during electropolymerization. Furthermore, films formed at a lower current density were more smooth and uniform, had a higher doping level, and were also more highly conducting. However, a steady decrease in strain over several oxidation and reduction cycles occurred regardless of the deposition current density, as pTS anions could partly move out the films, leading to less cation-driven actuation.

### References

1. Wang, J.; Chen, J.; Wang, C. Y.; Zhou, D.; Too, C. O.; Wallace, G. G. Synth Met 2005, 153, 117.
2. Larmat, F. R.; John, R.; Qiu, Y.-J. Synth Met 1996, 79, 229.

3. Cho, J.-H.; Yu, J.-B.; Kim, J.-S.; Sohn, S.-O.; Lee, D.-D.; Huh, J.-S. Sens Actuat B: Chem 2005, 108, 389.
4. Skaarup, S.; Bay, L.; West, K. Synth Met 2007, 157, 323.
5. Spinks, G. M.; Liu, L.; Wallace, G. G.; Zhou, D. Adv Funct Mater 2002, 12, 437.
6. Satoh, M.; Kaneto, K.; Yoshino, K. Jpn J Appl Phys Part 2: Lett 1985, 24, 423.
7. Khalkhali, R. A. Int J Chem Sci 2004, 2, 483.
8. Cheung, K. M.; Bloor, D.; Stevens, G. C. Polymer 1988, 29, 1709.
9. Heinze, J. Top Curr Chem 1990, 152, 1.
10. Smela, E. Adv Mater 2003, 15, 481.
11. Sabouraud, G.; Sadki, S.; Brodie, N. Chem Soc Rev 2000, 29, 283.
12. Tetsuji, H. S. Z.; Wataru, T. Bull Chem Soc Jpn 2005, 78, 506.
13. Ko, J. M.; Rhee, H. W.; Park, S. M.; Kim, C. Y. J Electrochem Soc 1990, 137, 905.
14. Satoh, M.; Imanishi, K.; Yoshino, K. J Electroanal Chem Interfac Electrochem 1991, 317, 139.
15. Satoh, M.; Kaneto, K.; Yoshino, K. Synth Met 1986, 14, 289.
16. Otero, T. F.; DeLaretta, E. Synth Met 1988, 26, 79.
17. West, K.; Jacobsen, T.; Zachau-Christiansen, B.; Careem, M. A.; Skaarup, S. Synth Met 1993, 55, 1412.
18. Okamoto, T.; Kato, Y.; Tada, K.; Onoda, M. Thin Solid Films 2001, 393, 383.
19. Kagawa, K.; Qian, P.; Tanaka, A.; Swager, T. M. Synth Met 2007, 157, 733.
20. Ochoteco, E.; Pomposo, J. A.; Bengoechea, M.; Grande, H.; Rodriguez, J. Polym Adv Technol 2007, 18, 64.
21. Jin, C.; Yang, F.; Yang, W. J Appl Polym Sci 2006, 101, 2518.
22. Smela, E. J Micromech Microeng 1999, 9, 1.
23. Ashrafi, A.; Golozar, M. A.; Mallakpour, S. Synth Met 2006, 156, 1280.
24. Iroh, J. O.; Su, W. J Appl Polym Sci 1997, 66, 2433.
25. Pytel, R.; Thomas, E.; Hunter, I. Chem Mater 2006, 18, 861.
26. Kiefer, R.; Chu, S. Y.; Kilmartin, P. A.; Bowmaker, G. A.; Cooney, R. P.; Travas-Sejdic, J. Electrochim Acta 2007, 52, 2386.
27. Maw, S.; Smela, E.; Yoshida, K.; Stein, R. B. Synth Met 2005, 155, 18.
28. Dyreklev, P.; Granstroem, M.; Inganaes, O.; Gunaratne, L. M. W. K.; Sendadeera, G. K. R.; Skaarup, S.; West, K. Polymer 1996, 37, 2609.
29. Chu, S. Y.; Kilmartin, P. A.; Jing, S.; Bowmaker, G. A.; Cooney, R. P.; Travas-Sejdic, J. Synth Met 2008, 158, 38.
30. Gandhi, M. R.; Murray, P.; Spinks, G. M.; Wallace, G. G. Synth Met 1995, 73, 247.
31. Li, Y.; Deng, B.; He, G.; Wang, R.; Yang, C. J Appl Polym Sci 2001, 79, 350.
32. He, X.; Shi, G. Sens Actuat B: Chem 2006, B115, 488.
33. Qu, L.; Shi, G.; Chen, F. E.; Zhang, J. Macromolecules 2003, 36, 1063.
34. Chen, W.; Li, C. M.; Chen, P.; Sun, C. Q. Electrochim Acta 2007, 52, 2845.
35. Chen, F. E.; Shi, G.; Fu, M.; Qu, L.; Hong, X. Synth Met 2003, 132, 125.
36. Crowley, K.; Cassidy, J. J Electroanal Chem 2003, 547, 75.
37. Liu, Y.-C. Electroanalysis 2003, 15, 1134.
38. Maddison, D. S.; Unsworth, J.; Roberts, R. B., Synth Met 1988, 26, 99.
39. Joo, J.; Lee, J. K.; Lee, S. Y.; Jang, K. S.; Oh, E. J.; Epstein, A. J., Macromolecules 2000, 33, 5131.
40. Kaynak, A. Mater Res Bull 1997, 32, 271.